Energy 67 (2014) 162–175

Contents lists available at ScienceDirect

Energy

journal homepage: www.elsevier.com/locate/energy

Assessment of maximum available work of a hydrogen fueled compression ignition engine using exergy analysis

Venkateswarlu Chintala, K.A. Subramanian*

Engines and Unconventional Fuels Laboratory, Centre for Energy Studies, Indian Institute of Technology, Delhi, New Delhi 110 016, India

ARTICLE INFO

Article history:
Received 6 August 2013
Received in revised form
23 January 2014
Accepted 26 January 2014
Available online 16 February 2014

Keywords:
Energy
Exergy
Hydrogen
Dual-fuel engine
Maximum available work
Irreversibility

ABSTRACT

This work is aimed at study of maximum available work and irreversibility (mixing, combustion, unburned, and friction) of a dual-fuel diesel engine (H_2 (hydrogen)–diesel) using exergy analysis. The maximum available work increased with H_2 addition due to reduction in irreversibility of combustion because of less entropy generation. The irreversibility of unburned fuel with the H_2 fuel also decreased due to the engine combustion with high temperature whereas there is no effect of H_2 on mixing and friction irreversibility. The maximum available work of the diesel engine at rated load increased from 29% with conventional base mode (without H_2) to 31.7% with dual-fuel mode (18% H_2 energy share) whereas total irreversibility of the engine decreased drastically from 41.2% to 39.3%. The energy efficiency of the engine with H_2 increased about 10% with 36% reduction in CO_2 emission. The developed methodology could also be applicable to find the effect and scope of different technologies including exhaust gas recirculation and turbo charging on maximum available work and energy efficiency of diesel engines.

1. Introduction

Diesel fuel consumption per capita for automotive diesel engines in the world increased drastically from 91.5 kg (oil equivalent) in 2003 to 125.5 kg in 2010 [1]. World demand for diesel engines is projected about 6.7% per year [2]. However, it emits high level of PM (particulate matter) and NO_x (oxides of nitrogen) emissions which are mainly due to the engine combustion with heterogenous air–fuel mixture. NO_x which forms at high temperature could decrease by reducing in-cylinder temperature but it decreases maximum available work resulting in increase in PM emission. EPA (Environmental Protection Agency) emphasized the emission regulation of diesel engine's PM that shall be evaluated based on diesel particulate size and count. The EPA emission regulations for Total Suspended Particles for $PM_{2.5}$ (fine particles indicator) and PM_{10} (coarse particles indicator) are 15 $\mu g/m^3$ and 100 $\mu g/m^3$ [3]. In case of European Countries, Euro-V emission regulation for PM emission of automotive diesel engines is 0.02 g/kWh which needs to be reduced further for Euro-VI emission regulation [4]. The future emission regulation for CI (compression ignition) engines targets CO_2 (Carbon dioxide) emission reduction along with other regulated emissions (CO (carbon monoxide), HC (hydro carbon), NO_x and PM (particulate count and size)). For example, European Union sets CO_2 emission regulation of 95 g/km by 2020 [5]. Environmental Protection Agency implemented CO_2 emission regulation (820 g/kWh) for light, medium and heavy duty vehicles for next three years (2014–16) [6]. The CO_2 emission from diesel engine can be reduced by energy efficiency improvement and carbon content reduction in fuel. The current technology for reducing emission from diesel engines is based on either temperature reduction (EGR (exhaust gas recirculation), retarding injection timing, etc.) or physical and chemical methods (selective catalytic reduction, diesel oxidation catalyst, etc). These technologies generally need energy input for their function resulting in reduction in maximum available work of the engine. Hence, green environment (less emissions of PM, and CO_2) and energy efficiency improvement are sustainable indicators of CI engines.

Utilization of H_2 (Hydrogen) in CI engines under dual-fuel mode could provide solutions to improve energy efficiency along with carbon-based emission reduction (CO, HC, PM and CO_2) as the engine with H_2 reduces the degree of heterogeneity ensuing to less PM emission (including its size and count) along with energy efficiency improvement and CO_2 emission reduction. Some studies reported the effect of H_2 on emissions (PM and CO_2) reduction and energy efficiency improvement of dual-fuel diesel engines. For example, Tsolakis reported that total particle number and total particle mass decreased from 0.55 cm^{-3} and 98.66 mg/cm^3 with

* Corresponding author.
E-mail addresses: subra@ces.iitd.ernet.in, subra@ces.iitd.ac.in (K.A. Subramanian).

0360-5442/$ – see front matter © 2014 Elsevier Ltd. All rights reserved.
http://dx.doi.org/10.1016/j.energy.2014.01.094

diesel to 0.37 cm^{-3} and 77.64 mg/cm^3 with 20% H_2 added EGR in a 8.6 kW direct injection diesel engine under dual-fuel mode at 1500 rpm and indicated mean effective pressure of 4.5 bar [7]. Wu et al. reported simultaneous reduction of CO_2, NO_x, and smoke emissions from a diesel engine (9.2 kW at 2400 rpm) under dual-fuel mode (diesel-gasoline) [8]. Miyamoto et al. reported CO_2 emission decreased from 688 g/kWh with base diesel fuel to 425 g/kWh with 10% H_2 (by volume) in a common rail direct injection diesel engine under dual-fuel mode [9]. Chintala and Subramanian reported energy efficiency of a diesel engine (7.4 kW) under dual-fuel mode increased about 5.4% with H_2 [10].

Hydrogen dual-fuel engine provides high fuel flexibility as it can operate in either conventional mode (diesel) or dual-fuel mode (diesel–H_2) depending on H_2 fuel availability. The existing NG (natural gas) infrastructure (storage, transportation and dispensing) could also be used for H_2 blended NG fuel. However, the existing system may need major modification for handling of H_2 (100%). For power generation and marine applications, the NG as main fuel is already being used in commercial dual-fuel diesel engines which are produced by diesel engine manufacturer including Cummins, Caterpillar and Wartsila. In the world, Delhi (India) is one of the largest vehicle fleet fueled with NG. The government of India is also taken further amendment by formulating fuel policy for implementation of H_2 blended natural gas (H_2: 18% by volume) as a fuel in IC (internal combustion) engines/vehicles [11]. National Hydrogen energy Roadmap (India) envisages road map for sustainable power generation and keeping air pollution free urban cities by utilization of H_2 as fuel for power generation (1000 MW aggregate capacity) and transport vehicles (one million) by 2020 [11]. A CI engine (at high compression ratio) could give higher energy efficiency with lesser CO_2 and PM emissions when it operates with H_2 fuel under dual-fuel mode as compared to spark ignition engine.

The energy efficiency of CI engine can be improved further by reducing the irreversibility and enhancing the available work from the system. In general, a CI engine produces irreversibility majorly due to combustion, air fuel mixing, wall heat transfer, exhaust gas, and friction. The literature status of these irreversibilities and available work from the engine systems is briefly described below.

1.1. Combustion irreversibility

Dunbar and Lior conducted a study of process irreversibility in an adiabatic combustion chamber and found one-third of the useful fuel energy is destroyed during combustion process [12]. Caton reported combustion irreversibility, which is mainly function of temperature, pressure and equivalence ratio, and it decreases with increasing combustion temperature [13]. But, Rakopoulos and Kyritsis reported the irreversibility is a function of fuel reaction rate as the combustion with lighter molecule fuels leads to decrease in irreversibility as compared to heavier molecule fuel [14]. Rakopoulos et al. reported that combustion process of the diesel engine fueled with H_2 (up to 10% by volume) produces less irreversibility under dual-fuel operation [15]. However, irreversibility produced during combustion in CI engines is not understood clearly so far.

1.2. Mixing irreversibility

Dunbar and Lior found the irreversibility of mixing of fuel with air is in the range of 8–10% of total reversibility [12]. Similarly, Jonathan and Dincer reported 9% of the total irreversibility which is produced by the mixing of fuel with air during suction stroke of a spark ignition engine [16]. As this mixing irreversibility is an important irreversible process, it needs to be studied for the dual-fuel diesel engine with H_2 fuel.

1.3. Wall heat transfer and exhaust gas losses

Taymaz reported that a diesel engine (136 kW at 2400 rpm) could decrease its heat transfer loss (through engine walls) from 27% without insulation to 23% with insulation. However, the heat loss increased through exhaust gases from 24% to 27% at higher load [17]. Information on irreversibility produced due to wall heat transfer and exhaust gas in CI engines is scanty in the literature. However, some researchers reported that the energy efficiency of the engine system could be improved by utilizing waste heat energy for application of combined heat and power (cogeneration) to industrial process because the energy losses typically through exhaust gas/cooling water from the engine. For example, Shu et al., studied the potential of waste heat recovery from a diesel engine using thermo-electric generator and organic cycle, and reported indicated thermal efficiency of the engine increased from 41% to 45.7% [18]. Ghazikhani et al., reported specific fuel consumption of multi cylinder direct injection diesel engine (85 hp at 2800 rpm) with exhaust gas recovery decreased about 10% [19]. Fu et al., reported energy efficiency improvement (about 6.3%) of a four cylinder CI engine (110 kW) using exhaust heat recovery. It is an interesting study that one cylinder (out of four) was operated by steam as working fluid which was generated using the heat input from waste exhaust gas energy of remaining three cylinders [20]. They also studied the potential of methanol as working fluid as well as fuel for combined cycle power plant (IC engine-ORC (organic rankine cycle)). Fu et al., reported methanol can be a working fluid for ORC system with efficiency improvement (3.9–5.2%) and subsequently, it is also utilized as fuel in IC engine for enhancing thermal efficiency (1.4–2.1%) [21]. Domingues et al., studied the potential of waste heat recovery from IC engine with ORC system with different working fluids (water, Hydrochlorofluorocarbons), and reported thermal efficiency and mechanical efficiency of the engine increased in the range of 1.4–3.52% and 10.16–15.95% [22]. The waste exhaust gas heat from IC engine was utilized for generating power (maximum net output of 2069 kW) in a ship using ORC with maximum energy and exergy efficiencies of 11% and 59% [23]. A diesel engine (20 kW) integrated with cogeneration system (heating, cooling and power) could significantly improve energy and exergy efficiencies [24]. Split cycle process was used for waste heat recovery from the marine engine and produced higher power output by 3.4% than conventional cycle [25]. Kalyan et al., concluded NO_x and CO_2 emission of a diesel engine with EGR decreased about 18% (on average) with ORC system [26]. ORC system with diesel engine (by combined cycle) has high potential to increase exergy (up to 21%) and energy efficiency (up to 6.1%) of the engine [27]. Sarabchi et al., studied utilization of waste heat from homogenous charge compression ignition for a tri-generation application (power, heating and cooling) and reported the second law efficiency of the tri-generation system is higher (about 5.19%) than the base engine [28]. It is clearly seen from the above discussion that the diesel engine with ORC/tri-generation system could enhance exergy efficiency of the engine but these systems (ORC/tri-generation) have limitation (additional system cost and complexity) on its usage in low rated power output system (automotive engine, and low and medium electrical power generation). Livio et al. reported that H_2 (8% by volume) blended NG fueled IC engine (65 kW rated power at 1500 rpm) with combined heat and power system could increase electrical efficiency significantly along with reduction of carbon monoxide and CO_2 about 27% and 9% [29]. There is no information in literature on wall heat transfer and exhaust gas energy loss of CI engines fueled with H_2.

1.4. Available work

Available work from CI engines is generally in the range of 25–40%. It can be increased with different technologies including dual-fuel strategy. Amjad et al. reported that available work increased from 32% with 44.6% NG mass fraction to 41% with 85.1% NG mass fraction under dual-fuel operation [30]. Yoge et al. also reported increase in available work from 35.4% with conventional diesel operation to 52.4% with NG based dual-fuel operation in a 188 kW diesel engine at 1800 rpm [31]. Harilal and Hitesh reported slight improvement in available work from 26% with base diesel operation to 28% with biogas based dual-fuel operation in a 5 kW diesel engine at 1450 rpm [32].

Brief review of energy and exergy balances of CI engine under dual-fuel mode (diesel with syngas, biogas and natural gas) is given in Table 1. A significant improvement in available work and reduction in irreversibility (except with syngas-diesel) could be obtained with dual-fuel operation (Table 1). However, information on irreversibility of H_2 based dual-fuel diesel engine is scanty in literature. Review of the literature on second law efficiency of dual-fuel engines shows that there is a large gap in finding exact reasons for exergy destruction and efficiency improvement with dual-fuel operation (diesel–H_2). Hence, a study is necessary to find out scope of energy efficiency improvement of H_2 fueled CI engine based on maximum available work. In this background, the present work is aimed at study of maximum available work and total irreversibility of a diesel engine under dual-fuel mode (diesel and H_2) using exergy analysis.

2. Model description

In the present study, dual-fuel engine is considered as an open system as mass and energy transactions occur between the system and surrounding. The other assumptions are that the system is under steady state and the working fluid follows ideal fluid law. The chemical energy of diesel (liquid) and H_2 (gas) is converted to heat energy during combustion and then converted it to shaft power (brake power).

2.1. Energy analysis

The input energy supplied by the fuels (diesel and H_2) to the dual-fuel engine system could be determined by using Eq. (1). The engine system delivers its output (shaft power) along with losses (wall heat transfer and exhaust gas) which could be determined by using Eqs. 2–10. Woshchni correlation can be used for calculating heat transfer coefficient as given in Eq. (10) [34].

$$\text{Input fuel energy}\left(E_{f,in}\right) = \dot{m}_{f1} \times CV_{f1} + \dot{m}_{f2} \times CV_{f2} \quad (1)$$

$$\text{Output shaft power}\left(P_{s,out}\right) = (2 \times \pi \times N \times T_r)/60 \quad (2)$$

$$\text{Output energy through exhaust gas}\left(E_{exh,out}\right) = \left(\dot{m}_{f1} + \dot{m}_{f2}\right) \times (1 + AF) \times C_{p\ exh,out} \times \left(T_{exh,out} - T_0\right) \quad (3)$$

$$\text{Air–fuel ratio(AF)} = \dot{m}_a/\left(\dot{m}_{f1} + \dot{m}_{f2}\right) \quad (4)$$

Heat transfer loss from burned gas to the system surrounding (atmosphere) occurs through three modes (conduction, convection and radiation) that could be determined by using Eqs. (5)–(8). Then the total heat transfer for all modes is calculated using Eq. (9).

$$\text{Heat loss through convection from burned gas to inner wall}\left(Q_{convection1,out}\right) = h_c \times A_r \times \left(T_g - T_{iw}\right) \quad (5)$$

$$\text{Heat loss through conduction from inner wall to outer wall}\left(Q_{conduction,out}\right) = K \times A_r \times \left(T_{iw} - T_{ow}\right) \quad (6)$$

$$\text{Heat loss through convection from outer wall to atmosphere}\left(Q_{convection2,out}\right) = h_c \times A_r \times \left(T_{ow} - T_0\right) \quad (7)$$

$$\text{Hea loss through radiation from burned gas to atmosphere}\left(Q_{radiation,out}\right) = b_z \times \left(T_g^4 - T_0^4\right) \quad (8)$$

$$\text{Total heat transfer}\left(Q_{t,out}\right) = Q_{convection1,out} + Q_{conduction,out} + Q_{convection2,out} + Q_{radiation,out} \quad (9)$$

$$\text{Convective heat transfer coefficient}\left(h_c\right) = 0.82 \times B^{-0.2} \times P^{0.8} \times V_g^{0.8} \times T^{-0.53} \quad (10)$$

It is assumed that the input energy of fuel is equal to sum of shat power, energy loss in exhaust gas, wall heat transfer loss and unaccounted losses. The engine power and its energy loss can be calculated by using Eqs. 11–15.

$$\text{Energy efficiency of shaft power} = \left(P_{s,out}/E_{f,in}\right) \times 100 \quad (11)$$

$$\text{Percentage of energy loss through exhaust gases} = \left(E_{exh,out}/E_{f,in}\right) \times 100 \quad (12)$$

Table 1
A review of energy and exergy balances in diesel engines.

S.No.	Author	Engine specifications	Fuel	Energy balance (in %)			Exergy balance (in %)			
				Power	Heat loss	Exhaust gas	Power	Heat loss	Exhaust gas	Irreversibility
1	Yoge et al. [31]	Cummins 6CTA $P = 188$ kW at 1800 rpm	Diesel	37.9	25.3	36.8	35.4	1.1	14.7	48.8
			Diesel + NG	55.1	13.1	31.8	52.4	0.06	12.7	34.3
2	Harilal and Hitesh [32]	$B = 95$ mm, $L = 90$ mm,	Diesel	28	35	37	26	7	16	51
		CR = 18:1 $P = 5$ kW at 1450 rpm.	Diesel + Biogas	28	38	34	28	8	17	47
3	Sahoo et al. [33]	Kirloskar TV1 $B = 87.5$ mm, $L = 110$ mm,	Diesel	–	–	–	19.8	4.9	16.4	58.9
		CR = 17.5:1 $P = 5.2$ kW at 1500 rpm.	Diesel + Syngas	–	–	–	18.3	0.4	16.1	65.2

Percentage of energy loss due to heat transfer

$$= \left(Q_{t,out}/E_{f,in}\right) \times 100 \quad (13)$$

Percentage of unaccounted energy loss

$$= \left(E_{unaccount,out}/E_{f,in}\right) \times 100 \quad (14)$$

Unaccounted energy loss$(E_{unaccount,out})$

$$= E_{f,in} - (P_{s,out} + E_{exh,out} + Q_{t,out}) \quad (15)$$

2.2. Exergy analysis

Exergy could be a tool to find out scope for improvement of energy efficiency of a thermal system. The quantification of maximum available work in a thermal system using exergy analysis would provide details including the order of exergy destructions and losses in the processes such as fuel vaporization, fuel air mixing, oxidation of reactant species, and friction. The stiochiometric combustion equation for dual-fuel engine is given in Eq. (16).

$$a_1\ C_{\alpha 1}H_{\beta 1} + b_1\ C_{\alpha 2}H_{\beta 2} + c_1(O_2 + 3.76N_2) \rightarrow d_1\ CO_2 + d_2\ H_2O + c_1 32.76\ N_2 \quad (16)$$

The details of atomic balance of carbon, hydrogen, and oxygen are given in Eqs. (17)–(23).

$$a_1 = \dot{M}_{f1}/\left(\dot{M}_{f1} + \dot{M}_{f2}\right) \quad (17)$$

$$b_1 = \dot{M}_{f2}/\left(\dot{M}_{f1} + \dot{M}_{f2}\right) \quad (18)$$

$$\dot{M}_{f1} = \dot{m}_{f1}/MW_{f1} \quad (19)$$

$$\dot{M}_{f2} = \dot{m}_{f2}/MW_{f2} \quad (20)$$

$$c_1 + (a_1 \times \alpha_1 + b_1 \times \alpha_2) + (a_1 \times \beta_1 + b_1 \times \beta_2)/4 \quad (21)$$

$$d_1 = a_1 \times \alpha_1 + b_1 \times \alpha_2 \quad (22)$$

$$d_2 = (a_1 \times \beta_1 + b_1 \times \beta_2)/2 \quad (23)$$

Chemical availability of fuel can be determined using Gibbs free energy as given in Eqs. (24) and (25) [35].

Chemical availability of fuel$\left(A_{f,in}\right) = \Delta G_{f(T_0,P_0)}$

$$= \hat{g}Pr_{(T_0,P_0)} - \hat{g}R_{(T_0,P_0)} \quad (24)$$

$$A_{f,in} = a_1 \times \hat{g}_{f1(T_0,P_0)} + b_1 \times \hat{g}_{f2(T_0,P_0)} + c_1 \times \hat{g}O_{2(T_0,P_0)} - \left[d_1 \times \hat{g}CO_{2(T_0,P_0)} + d_2 \times \hat{g}H_2O_{(T_0,P_0)}\right] + R_u \times T_0 \times \ln\left\{(\dot{x}_{O_2})^{c1}/\left[(\dot{x}_{CO_2})^{d1} \times \left((\dot{x}_{H_2O})^{d2}\right)\right]\right\} \quad (25)$$

where $\dot{x}_{O_2}$, $\dot{x}_{CO_2}$, and $\dot{x}_{H_2O}$ represent mass fractions of corresponding species those can be determined using Eqs. (26)–(28).

Mass fraction of oxygen$(\dot{x}_{O_2}) = \dfrac{(n_{O_2} \times MW_{O_2})}{\sum_i n_i \times MW_i}$ (26)

Mass fraction of $CO_2(\dot{x}_{CO_2}) = \dfrac{(n_{CO_2} \times MW_{CO_2})}{\sum_i n_i \times MW_i}$ (27)

Mass fraction of Water$(\dot{x}_{H_2O}) = \dfrac{(n_{H_2O} \times MW_{H_2O})}{\sum_i n_i \times MW_i}$ (28)

Exergy (availability) transfer (in the form of work and heat) is determined using Eqs. (29) and (30).

Availability of output shaft power$(A_{s,out}/d\theta)$

$$= \int_1^2 (p - p_0) \times \frac{dv}{d\theta} \quad (29)$$

Availability of cylinder wall heat transfer$\left(A_{Q_{t,out}}\right)$

$$= \int_1^2 Q_{t,out} \times \left(1 - \frac{T_0}{T_g}\right) \quad (30)$$

Flow availability of exhaust gas can be determined using Eq. (31) [36].

$$A_{exh,out} = \sum x_i\{h_i(T) - h_i(T_0) - T_0[s_i(T) - s_i(T_0)]\} + \sum R_u T_0 \ln\left(\frac{x_i p}{x_{io} p_0}\right) \quad (31)$$

Percentage of work availability of the engine, availability transfer through exhaust gases and wall heat transfer, and total irreversibility can be calculated by using Eqs. (32)–(35).

Percentage of work availability $= \left(A_{s,out}/A_{f,in}\right) \times 100$ (32)

Percentage of exhaust gas availability

$$= \left(A_{exh,out}/A_{f,in}\right) \times 100 \quad (33)$$

Percentage of heat transfer availability $= \left(A_{Q_{t,out}}/A_{f,in}\right) \times 100$ (34)

Percentage of total irreversibility $= \left(I_t/A_{f,in}\right) \times 100$ (35)

3. Experimental setup

A single cylinder four-stroke diesel engine was chosen for conducting the experiments for this study. A schematic diagram of the experimental setup is shown in Fig. 1 and the technical specifications of the engine are given in Table 2. Pilot fuel (diesel) was injected using the engine's conventional injection system whereas the gaseous fuel (H_2) was injected using auxiliary injection system which was controlled by an electronic control unit. Hydrogen was injected into the intake manifold after the outlet valve closed (43° crank angle ATDC (after top dead center)) in order to avoid scavenging losses. The engine system was instrumented with gas mass flow meter for measurement of gaseous fuel flow rate, and electronic weighing balance for liquid fuel flow

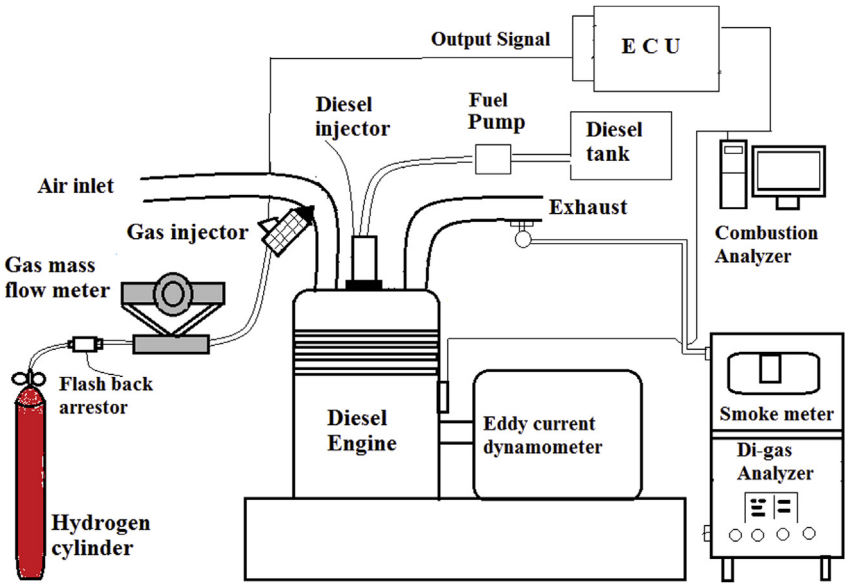

Fig. 1. Schematic diagram of experimental setup.

rate. In-cylinder pressure and diesel fuel line pressures with respect to crank angle data were captured by Indicom system which comprised of in-built charge amplifier, data acquisition system. Post processing software system was used for processing the pressure-crank angle data and inline fuel injection pressure (diesel). Experimental tests were conducted on the engine under dual-fuel mode with diesel (pilot fuel) and H_2 fuels at 50%, 75%, and 100% loads at constant engine speed of 1500 rpm. Uncertainty values of shaft power output, fuel flow rate and energy efficiency are determined using Eq. (36) [37] and their values are given in Table 3. Properties of fuels used in the study are given in Table 4. The measured experimental data are given as input to the exergy equations for calculating maximum available work and irreversibility of the system. Some results of exergy analysis are validated with the experimental data which were measured for this study and also taken from literature.

$$q = \left[\left(\frac{\partial q}{\partial x_1}\Delta x_1\right)^2 + \left(\frac{\partial q}{\partial x_2}\Delta x_2\right)^2 + \ldots\ldots\ldots + \left(\frac{\partial q}{\partial x_n}\Delta x_n\right)^2\right]^{\frac{1}{2}} \quad (36)$$

Table 2
Technical specifications of the engine.

S.No.	Parameter	Description
1	Make and Model	Kirlosker and EA10
2	Number of cylinders	1
3	Displacement volume, cc	947.4
4	Rated power output, kW	7.4
5	Rated speed, rpm	1500
6	Bore × Stroke, mm	102 × 116
7	Compression ratio	19.5:1
8	Connecting rod length, mm	232.6
9	Intake valve opening and closing, degree crank angle	43 BTDC and 67 ABDC
10	Exhaust valve opening and closing, degree crank angle	87 BBDC and 39 ATDC

4. Results and discussion

4.1. Energy conversion balance

4.1.1. Effect of H_2 addition on energy efficiency

The percentage of H_2 energy substitution in diesel engine under dual-fuel mode is limited due to knocking problem. It is observed from the present study that knock-limited H_2 energy shares for the diesel engine under dual-fuel mode are 48%, 33.6%, and 18% for 50%, 75%, and 100% loads. But, in literature, the optimum energy shares are reported differently. For example, Horng and Zhan [38] observed better fuel consumption and lower emissions with 20% H_2 share in a diesel engine (9.2 kW) at 2400 rpm as compared to base diesel value.

Fig. 2(a) shows conversion of fuel chemical energy to shaft power output (brake power) in a H_2 fueled dual-fuel engine at constant engine speed of 1500 rpm. Energy efficiency (Brake thermal efficiency) increases significantly with increasing H_2 energy share as shown in the figure. It increased from 31.6% with conventional diesel fuel operation to 34.8% with dual-fuel mode operation (18% H_2 energy share) at rated load. This could be due to better

Table 3
Uncertainty values of various parameters.

S.No.	Parameter	Uncertainty (%)
1	Shaft power output	0.19
2	Energy efficiency of shaft power	0.25
3	Mass flow rate of air	1.7
4	Mass flow rate of diesel	2.3
5	Mass flow rate of hydrogen	1.4
6	Exhaust gas temperature	0.166
7	Output energy through exhaust gas	2.147
8	Heat transfer loss	2.432
9	Chemical availability of fuel	1.999
10	Availability of shaft power	3.284
11	Availability of heat transfer	2.95
12	Availability of exhaust gas	3.312
13	Fuel air mixing irreversibility	1.58
14	Combustion irreversibility	1.127
15	Irreversibility due to unburned fuel	2.642
16	Friction irreversibility	2.3

Table 4
Properties of diesel and hydrogen fuels.

S.No	Fuel characteristics	Diesel	Hydrogen
1	Lower heating value, MJ/kg	43.6	120
2	Stiochiometric air–fuel ratio	14.5	34.2
3	Energy density at 15 °C and 100 kPa, MJ/m^3	35.8	10.3
4	Auto ignition temperature, K	530	858
5	Laminar burning velocity, m/s	0.3	2.65–3.25
6	Flammability limits (%volume in air)	0.7–5	4–75
7	Minimum ignition energy, mJ	–	0.02
8	Density at 15 °C and 100 kPa, kg/m^3	848	0.083
9	Diffusivity in air, cm^2/s	0.038	0.63

combustion with the addition of H_2 fuel to diesel fueled CI engine. The reasons for the increase in efficiency are better mixing of fuel with air due to higher diffusivity of H_2 (0.63 cm^2/s) and the higher peak temperature (2014 K at rated load) as compared to base diesel mode. The cumulative heat release rate increases correspondingly with increasing combustion temperature. Carnot efficiency of the engine (Carnot efficiency $= 1 - (T_{low}/T_{peak})$) is directly proportional to peak temperature. The peak temperature (Fig. 3) of the dual-fuel engine increases that result in higher Carnot efficiency and energy efficiency as compared to base mode operation. High temperature combustion also enhances the oxidation of intermediate species (HC, CO, and soot). In diesel engines, different air–fuel ratios are

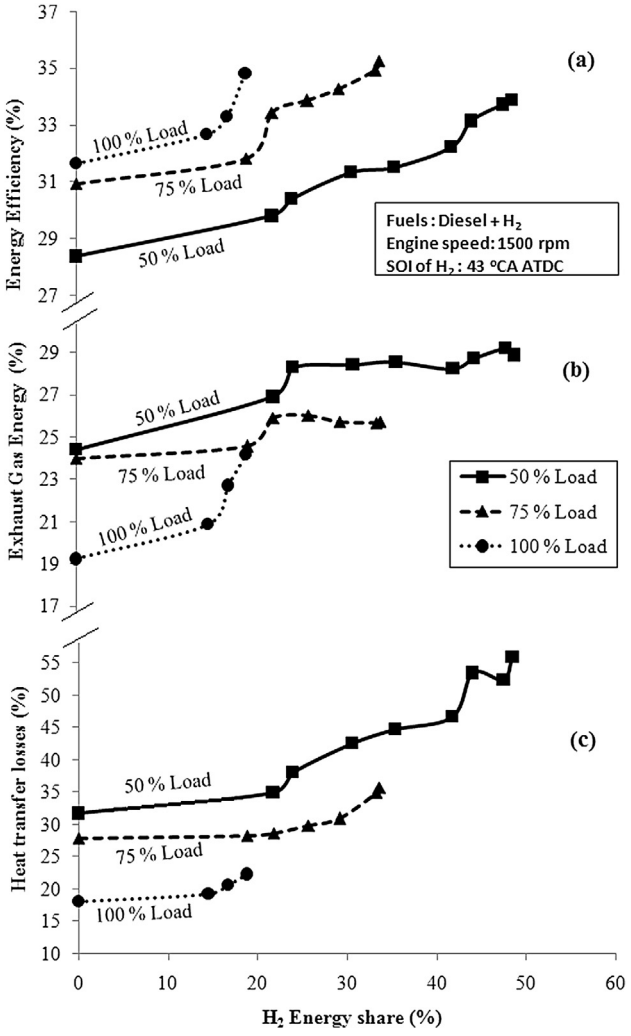

Fig. 2. Energy distribution with respect to H_2 energy share.

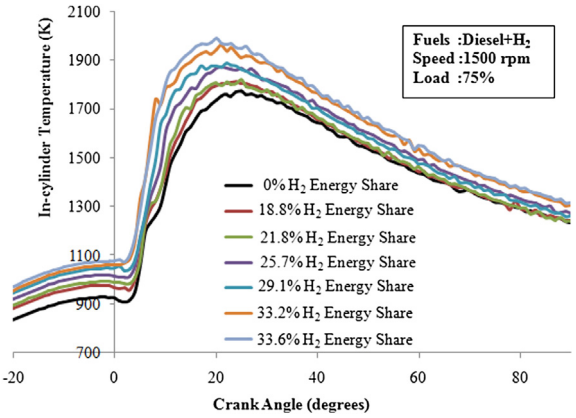

Fig. 3. In-cylinder temperature with respect to degree crank angle.

generally formed and distributed heterogeneously and mixture strength varies from perpendicular to centre of cylinder axis to wall at a given crank angle position. The mixture strength would be generally in stoichiometric or slightly rich in around the fuel spray whereas it is too lean in near cylinder wall. If the air–fuel ratio is beyond the flammability limit, ignition and combustion will not occur resulting in formation of unburned HC and CO. In case of H_2, flammability limit (4–75% volume in air) is wider than base diesel (0.7–5% volume in air) leading to better oxidation of fuel which enhances energy efficiency of the engine. In addition to this, H_2 fuel, which is in gaseous state for a typical engine operating condition, enhances the degree of homogeneity of air–fuel mixture in the engine's combustion chamber. Hence, combustion efficiency and energy efficiency increase significantly with H_2. However, first law of thermodynamics is unable to find out the particular reason for efficiency improvement and also quantitative analysis. Hence, the system needs the exergy analysis based on second law of thermodynamics which is explained in Section 4.2.

4.1.2. *Effect of H_2 addition on exhaust gas energy*

Percentage of energy loss from exhaust gas increases significantly with increasing H_2 energy share as shown in Fig. 2(b). It decreases with increase in engine load resulting in higher energy efficiency at higher load. It may be noted that exhaust gas temperature is higher with higher load as compared to lower load but percentage of exhaust gas energy is lesser for higher load. Exhaust gas energy, which is strongly dependent on exhaust gas temperature, is given in Eq. (3). If the exhaust gas temperature increases, its energy loss also increases. As H_2 has higher heat content (120 MJ/kg) than base diesel (42.5 MJ/kg), the combustion temperature increases that leads to high exhaust gas temperature. Exhaust gas energy increased from 24% with base diesel to 25.7% with 33.6% H_2 energy share at 75% load.

4.1.3. *Effect of H_2 addition on heat transfer losses*

Heat transfer loss occurs mainly through the engine components (cylinder head, inlet and exhaust valves, and cylinder walls). Total heat transfer loss from burned gas to engine component (system surrounding) increased from 27.8% with base diesel to 35.7% with 33.6% H_2 energy share along with diesel fuel at 75% load (Fig. 2(c)). It is found among three modes of heat transfer (conduction, convection, and radiation) that convective heat transfer for fuel oxidation zone to dead state zone is to be a dominant mode. Heat energy loss is directly proportional to in-cylinder combustion temperature as it increases with increase in the temperature and vice versa. So, a conclusion is emerged from the above analysis that

the wall heat transfer loss is higher with diesel–H_2 dual-fuel mode than conventional mode of the engine operation.

In general, increase in energy loss of any thermal system would lead to decrease in energy efficiency. But it can be observed from Fig. 2(c) that energy efficiency with H_2 increases even though increase in energy losses (exhaust and wall heat transfer). Thus, analysis of thermal system using first law of thermodynamic does not provide the complete and exact reason for the efficiency improvement. In addition to this, it is unable to analyze frictional loss which is one of the major losses in internal combustion engines. Furthermore, first law is unable to find the maximum work that can be extracted from the engine system. Hence, second law analysis is required to find out the maximum work available in the engine system and also identify the avenues for further improvement.

4.2. Exergy conversion balance

4.2.1. Effect of H_2 addition on maximum available work

Availability or exergy is the maximum useful work that can be extracted from the system when it is attained to thermal, mechanical and chemical equilibrium with environment. Maximum wok can be extracted when a system attains the change in entropy is zero. Fig. 4 shows work availability (exergy efficiency of shaft work output) for different H_2 energy shares at different loads and constant engine speed (1500 rpm). Work availability increased from 29.1% with base diesel to 31.7% with 18% H_2 energy share at rated load as shown in the figure. The work availability could be increased significantly with high amounts of H_2 energy shares. For example, work availability increased from 27% with base diesel to 31.8% with 48.4% H_2 energy share at 50% load. However, H_2 addition with high-energy share to the diesel engine under dual-fuel mode is limited by knocking problem.

It could be observed from Fig. 4 that work availability increases with increasing engine load. For base diesel operation, it increased from 27% at 50% load to 28.3% at 75% load and 29.1% at 100% load. The reason for the higher work availability is due to increase in combustion efficiency by decrease in total irreversibility of the system as compared to conventional mode and the detailed explanation is given in Section 4.2.5.

Fig. 5 represents the variation of specific energy consumption (SEC) with H_2 energy share. The SEC decreases significantly with increasing H_2 energy share as it decreased from 11.4 MJ/kWh with base diesel to 10.4 MJ/kWh with 18% H_2 energy share at 100% load. For a given output power, input energy (specific energy consumption) decreases with increasing H_2 energy share that enhances the work availability. These results have good agreement with the work reported by Jonathan and Dincer [16].

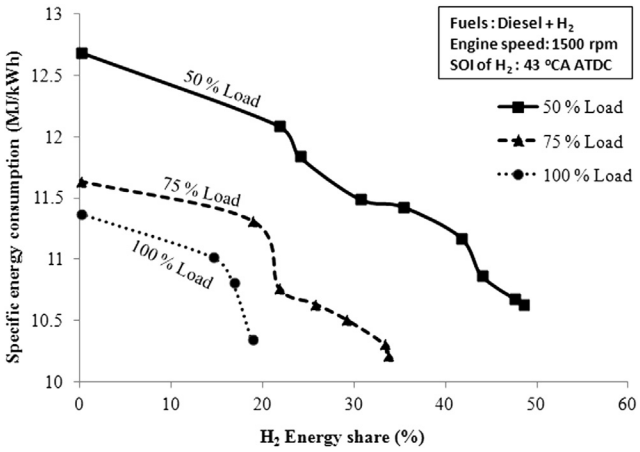

Fig. 5. Specific energy consumption variation with respect to H_2 energy share.

Reaction rate of any fuel can be determined using Arrhenius Eq. (37). It is evident from the equation that fuel oxidation rate is directly proportional to combustion temperature. This reaction rate increases exponentially with increasing in-cylinder temperature during combustion. As combustion temperature increases with increasing H_2 energy share, reaction rate increases exponentially resulting to significant improvement in combustion efficiency.

$$RR = k_1 \times \exp(-E_a/R_u T) \times [\text{Fuel}]^{k_2} \times [\text{Oxidizer}]^{k_3} \quad (37)$$

4.2.2. Effect of H_2 addition on exhaust gas availability

Fig. 6 shows availability from exhaust gas and heat transfer with increasing H_2 energy share in the dual-fuel engine for different loads. Exhaust gas availability decreases moderately with increasing H_2 energy share at all loads as shown in the figure. The reason for the decrease in the availability could be due to no significant change in composition and properties of burned species with increase of H_2 energy share. Exhaust gas availability decreased from 17.2% with base diesel to 15.4% with 33.6% H_2 energy share under dual-fuel mode at 75% load. However, exhaust gas

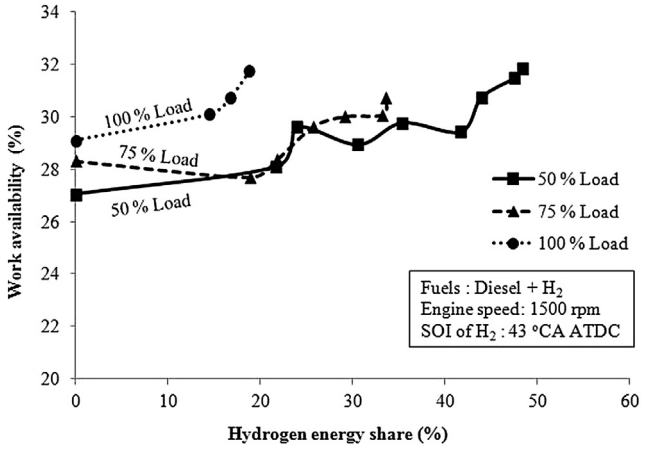

Fig. 4. Work availability variation with respect to H_2 energy share.

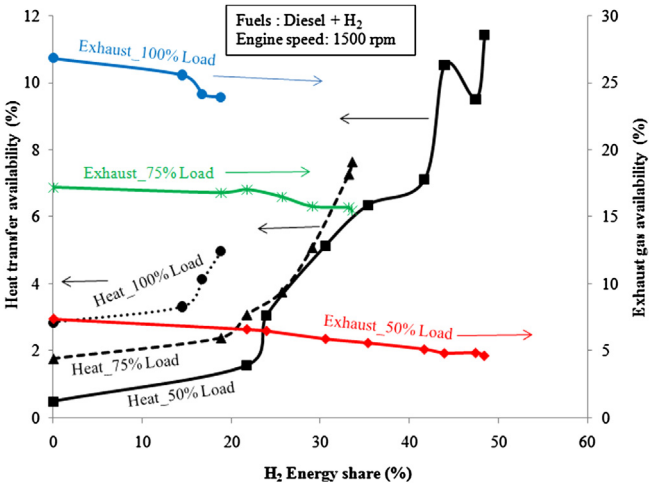

Fig. 6. Availability transfer through exhaust gas and heat transfer.

availability increases drastically with increase in engine load. For example at 18% H_2 energy share, it increased from 6% with 50% load to 16.7% with 75% load and further to 24% with 100% load.

4.2.3. Effect of H_2 addition on availability transfer through heat

Availability from wall heat transfer increases substantially with increasing H_2 energy share as shown in Fig. 6. It increased from 1.7% with conventional diesel operation to 7.6% with 33.6% H_2 energy share under dual-fuel operation at 75% load as shown in the figure. Heat availability could be determined using Eq. (30) which indicates that it is directly proportional to in-cylinder combustion temperature. Maximum combustion temperature increased from 1805.2 K with diesel operation to 1987.2 K with 33.6% H_2 energy share in dual-fuel mode operation as shown in Fig. 3. As combustion temperature increases, heat availability also increases. Caton also reported the similar trend that heat availability increased with high temperature combustion [13].

4.2.4. Total irreversibility classification

Availability is not a conservative property because it may be destroyed by irreversibility due to the process such as combustion, heat transfer through a finite temperature difference, friction, or mixing process. Some researchers classified the total irreversibility of the engine system into sub-processes. For example, Dunbar and Lior divided the irreversibility for oxidation of fuel into three sub-processes: (i) fuel oxidation, (ii) heat transfer, and (iii) mixing process [12]. Similarly, Prins and Ptasinski also classified the irreversibility for oxidation process into three sub-processes: (i) instantaneous chemical reaction (ii) heat transfer from intermediate products to reactants and (iii) mixing. They reported that at stoichiometric combustion, exergy losses due to heat transfer (14–16%) are higher than chemical reaction (9–11%) [39]. Jonathan and Dincer divided the total irreversibilities into three sub-process and reported that 77% of the total irreversibility is caused by preheating of air in the intake manifold and main heating during the compression stroke. About 14% and 9% of the total irreversibility are caused by the combustion reaction and mixing of reactants in the intake manifold [16]. Salehzadeh et al., analyzed a diesel engine with tri-generation system using the exergy destruction of every component of cooling, heating and power system, and reported the performance (first and second law efficiency) of the engine increased significantly with tri-generation system [40]. Hongqing and Huijie studied the effect of start of combustion and combustion duration on irreversibilities due to combustion and heat transfer in a spark ignition engine with compression ratio of 9:1 [41]. At the same start of combustion, the combustion irreversibility decreases with increase in combustion duration whereas heat transfer irreversibility increases. They found the total combustion irreversibility was about 19% during the fuel oxidation. Rakopoulos et al., investigated the degree of reversibility of the combustion process in all burned zones of a turbocharged spark ignition engine and concluded that the combustion temperature is the main dominating factor which effects the combustion irreversibility [42].

Though some researchers studied the irreversibility in single fuel based combustion process, information of irreversibility in dual-fuel combustion is not available in the literature. Hence, in this study, in order to assess the major irreversibility occurring in the dual-fuel engine system, the total irreversibility in the dual-fuel engine system is classified into four types of irreversibilities: (i) irreversibility due to air fuel mixing, (ii) combustion irreversibility, (iii) friction irreversibility, and (iv) irreversibility due to unburned fuel as shown in Fig. 7.

4.2.4.1. Irreversibility due to air fuel mixing. Irreversibility due to air fuel mixing during suction, compression and combustion processes

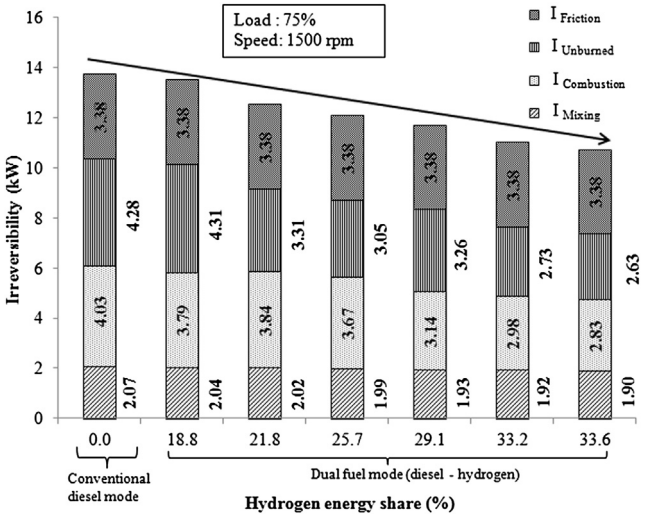

Fig. 7. Total irreversibility classification in diesel engine.

is determined using Eq. (38). In case of conventional diesel engine (single fuel), mixing irreversibility occurs only during injection period in compression and combustion processes whereas in dual-fuel operation the irreversibility occurs in all three processes (suction, compression, and combustion) as main fuel (H_2) and pilot fuel (diesel) are to be injected during suction and compression stroke respectively.

$$\text{Irreversibility due to fuel air mixing}(I_{\text{mixing}}) = -R_u \times T_0 \times \sum_i \dot{m}_i \times \sum_i n_i \times \sum_i (x_i \times \ln(x_i)) \quad (38)$$

Mixing irreversibility decreases with increasing H_2 energy share (Fig. 7). This reduction is due to increase in gaseous fuel (H_2) concentration with corresponding decrease in liquid fuel (diesel) concentration under dual-fuel operation. For instance, mole fraction of liquid diesel fuel decreased significantly from 0.0064 with base diesel mode to 0.0038 with dual-fuel mode (33.6% H_2 energy share) at 75% load. Gaseous fuel can mix with air rapidly due to its higher diffusivity (H_2 diffusivity: 0.63 cm^2/s) property than liquid fuel (diesel diffusivity: 0.038 cm^2/s) resulting to the irreversibility reduction. The mixing irreversibility decreased from 2.07 kW with base diesel to 1.9 kW with 33.6% H_2 energy share under dual-fuel mode at 75% load. Rakopolus et al., also reported the same trend that irreversibility in mixing during H_2 combustion is lesser than liquid hydrocarbon fuel combustion [15].

4.2.4.2. Combustion irreversibility. Irreversibility in oxidation/combustion process is determined using Eq. (39). It decreases significantly with increasing H_2 energy share under dual-fuel operation as shown in Fig. 7. It decreased from 4.03 kW with base diesel to 2.83 kW with 33.6% H_2 energy share at 75% load.

$$\text{Irreversibility due to combustion}(I_{\text{combustion}}) = T_0 \times \sum_{fi} \dot{m}_i \times \left\{ s_0 + C_p \ln\left(\frac{T}{T_0}\right) - R_u \ln\left(\frac{P}{P_0}\right) \right\} \quad (39)$$

The entropy generation decreases during the combustion process with increasing H_2 energy share which leads to reduction in combustion irreversibility. Entropy generation during combustion decreased from 795.4 J/kg K with base diesel operation to 581.1 J/kg K with 33.6% H_2 energy share at 75% load. This reduction is mainly due to increase in combustion temperature by high flame

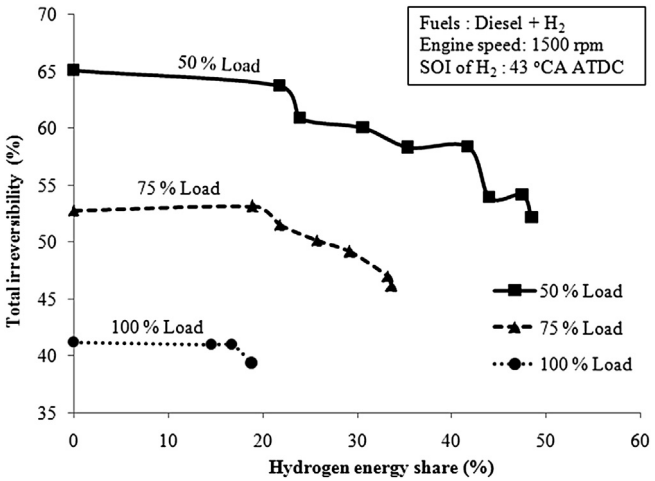

Fig. 8. Total irreversibility variation with respect to H_2 energy share.

velocity and high heat content of H_2 fuel. Alta et al., found about 6–9% reduction in entropy generation due to increase in combustion temperature about 100 K [43]. These experimental results confirm the results reported by Caton that irreversibility during combustion decreases if the combustion occurs at high temperature [13]. Jonathan and Dincer also reported that the combustion irreversibility decreases with the H_2 fueled IC engine as compared to gasoline [16].

4.2.4.3. Irreversibility due to unburned fuel. The chemical availability of input fuel is wasted if the whole fuel is not fully oxidized during combustion. Amount of unburned hydrocarbon directly indicates the amount of unavailable work from the engine system. Irreversibility due to the unburned fuel is calculated using Eq. (40).

$$\text{Irreversibility due to unburned fuel}(I_{\text{unburned}}) = \oint \left(\mathrm{d}\dot{m}_{\text{unburned}} \times A_{\text{f,in}}\right)\mathrm{d}\theta \tag{40}$$

From the above equation, it can be concluded that unburned fuel irreversibility is directly proportional to the amount of unburned fuel. As the quantity of unburned fuel decreases with H_2 addition, unburned fuel irreversibility decreases significantly with increasing H_2 energy share as shown in Fig. 7. High flame propagation of H_2 promotes the rapid combustion and enhances degree of complete combustion (combustion efficiency). The increase in combustion efficiency leads to reduction in quantity of unburned fuel. Unburned fuel irreversibility decreased from 4.28 kW with pure diesel fuel to 2.63 kW with 33.6% H_2 energy share under dual-fuel operation at 75% load. This reduction is also due to decrease in ignition energy of mixture (H_2 + diesel + air) and increase in combustion temperature with H_2. Combustion temperature increases significantly due to production of less number of carbon-based intermediate species including CO, CO_2, unburned hydrocarbons, and soot which absorb less amount of specific heat during oxidation process. Irreversibility decreases with H_2 which has inherent property including high flame velocity and high heat content resulting to better combustion and higher heat release rate as compared to diesel fueled conventional CI engine.

4.2.4.4. Irreversibility due to friction. Frictional loss is a strong function of engine speed. It can be calculated using Eqs. (41) and (42). The amount of frictional power is directly proportional to frictional irreversibility. In present study, as the entire experimental tests were conducted on the diesel engine at constant speed of 1500 rpm, it is assumed that there is no change in frictional irreversibility for both modes (conventional and dual-fuel mode) as shown in Fig. 7. However, the same methodology could also be applicable for variable speed automotive engines. For automotive engines, friction irreversibility varies depending upon the speed of the engine.

Frictional power with respect to degree crank angle is determined using Eq. (41).

$$fp(\theta) = \mu \times \left\{ \frac{\pi LN}{60} \operatorname{Sin}\theta \left[\frac{\operatorname{Cos}\theta}{\sqrt{R_l^2 - \operatorname{Sinn}^2\theta}} \right] \right\}^2 \tag{41}$$

Total cyclic frictional power or frictional irreversibility (I_{friction}) is calculated using Eq. (42).

$$FP_{\text{u}}(\theta) = \oint fp_{(\theta)}\mathrm{d}\theta = I_{\text{friction}} \tag{42}$$

It may be noted that smoke/soot enters into the lubricating oil during combustion and early part of expansion process. The soot particles have diameters in the range of 0.01–0.9 μm after

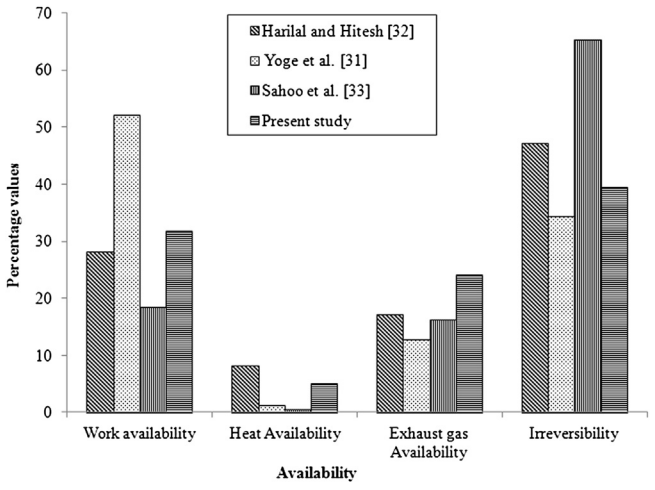

Fig. 9. Comparison of some exergy results with literature data.

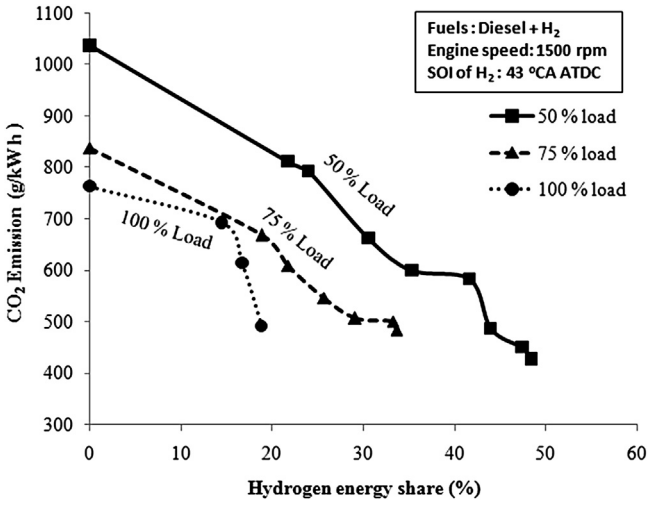

Fig. 10. CO_2 emission variation with respect to H_2 energy share.

combustion. As the oil film thickness in boundary lubrication is thinner (0.001–0.05 μm) than soot particles that leads to abrasive wear of engine components. In case of hydrodynamic lubrication, the lubricating films are normally many times thicker (5–500 μm) than the height of the irregularities on the bearing surface resulting in no problem of abrasive wear. In case of mixed lubrication, the oil film may be of hydrodynamic, partial film, or thin film (0.5–2.5 μm) which leads to wear of the engine components. Some studies were reported the effect of soot/smoke contaminated lubricating oil on wear of engine components. For example, Antusch et al. found that the wear rate increases with the soot particulate concentration in the oil. They also reported that apart from soot concentration, other factors including morphology, surface chemistry, and reactivity of the soot influence the wear rate of the engine components. This is due to particulates are not abrasive but they offer reaction sites for mechanochemical interaction [44]. Truhan et al. found that the soot concentration in oil has significant effect on liner wear but no effect on ring wear. They also reported the liner wear rate increased from 1.5 μm/h with 2% by weight soot content to 4.7 μm/h with 8% by weight soot content [45]. Staley found that the engine wear (on components: bearings, piston rings and cylinder liners) decreased about 50% and 70% with reduction of contaminants in the oil using 30 micron and 15 micron filtration respectively [46]. Soot could change the morphology of lubricating oil that would affect frictional power. Even though full substitution (100%) of hydrogen could not generally possible due to limitation of knocking, the partial substitution of H_2 in a diesel engine under dual-fuel mode could significantly reduce soot/smoke emission (Fig. 11) resulting in reduction in frictional power. However, combustion temperature of the engine with hydrogen is higher than base diesel resulting in increase in lubricating oil temperature which could increase frictional power. Green et al., investigated the effect of soot (carbon black) contaminated lubricants in the wear process of a simulated engine valve train contact and concluded that wear increases with increase in soot contamination of lubricating oil. However, the wear levels increase significantly with increasing temperature due to reduced oil film thicknesses [47]. Therefore, the net gain of its effect on frictional power needs to be studied as a future work. It is observed from this study that the frictional power of the engine with hydrogen (18.8%–33.6% energy share) at 75% load is in the range of 3.13–3.35 kW as compared to base diesel (3.73 kW) with uncertainty of 2.3%. However, the long endurance test is needed in order to confirm the effect of soot on performance of lubricants and frictional power of the engine.

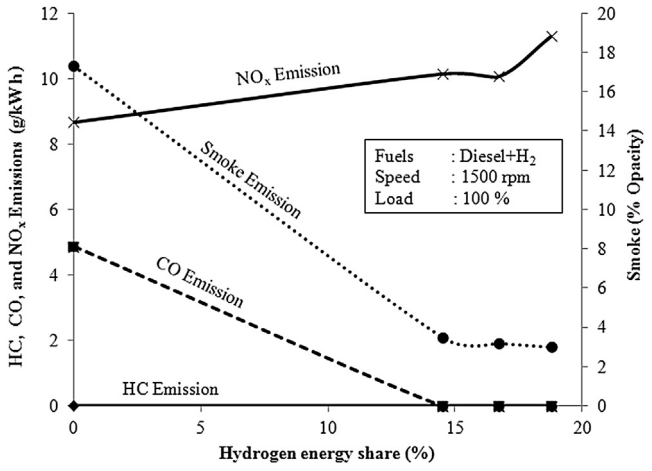

Fig. 11. Smoke, HC, CO, and NO_x emissions with respect to H_2 energy share.

4.2.5. Total irreversibility reduction

Total irreversibility produced in the system is determined using Eq. (43). Fig. 8 shows the total irreversibility at different loads with variation of H_2 energy share under dual-fuel operation. It decreases with increasing load as shown in the figure. For example, at 18% H_2 energy share under dual-fuel operation, it decreased from 63.7% with 50% load to 53% with 75% load and further to 39% with 100% load. These results have good agreement with the results reported by Rakopolous and Giakoumis that irreversibility decreases with increasing engine load [48]. They concluded that total irreversibility decreases due to decrease in combustion irreversibility with increasing load. The amount of combustion irreversibility depends on the fuel–air equivalence ratio. As the load increases, equivalence ratio increases that leads to enhance the in-cylinder temperature in combustion chamber resulting in reduction in combustion irreversibility.

$$\text{Total irreversibility}(I_t) = I_{\text{mixing}} + I_{\text{combustion}} + I_{\text{unburned}} + I_{\text{friction}} \quad (43)$$

Total irreversibility decreased from 52.7% with conventional diesel operation to 46.2% with 33.6% H_2 energy share at 75% load. This could be attributed due to significant reduction in irreversibility of unburned fuel and combustion as shown in Fig. 7. Increase of H_2 energy share leads to enhancement of degree of complete combustion and subsequently reduces the unburned products. Rakopolus et al., also concluded that irreversibility decreases with addition of H_2 as compared to conventional fuel [15]. It may be noted that entropy generation due to combination simple molecules into a more complicated one (Eq. (44)) is higher than the destruction of complex molecule into many number of lighter species (Eq. (45)). Hence entropy generation decreases with H_2 fuel combustion under dual-fuel mode of engine operation.

$$H_2 + 0.5O_2 \rightarrow H_2O \quad (44)$$

$$C_{16}H_{34} + 24.5(O_2 + 3.76N_2) \rightarrow 16CO_2 + 17H_2O + 92.12N_2 \quad (45)$$

4.3. Comparison of energy and exergy balances

Table 5 gives the comparison between energy and exergy balances according to first and second law of thermodynamics for the dual-fuel engine with 33.6% H_2 energy share. Table 6 gives the summary of first and second law analysis applied to dual-fuel engine. It can be observed from Table 5 that there is large difference between first and second law analysis on energy loss in heat transfer and exhaust gas. As the first law describes only two major losses, the law does not provide to find out scope for further improvement of energy efficiency of the system. From the second law analysis, an important conclusion is emerged from this study that there is a scope for further reduction of irreversibility of the dual-fuel engine by reducing combustion irreversibility and unburned fuel irreversibility. This is one of the main outcomes of this study.

Fig. 9 shows the validation of some exergy results of the dual-fuel engines (with different gaseous fuels) with the available data in literature. Exhaust gas availability and irreversibility are comparable with other studies. However, work availability and heat availability do not match with the literature data. The developed methodology of exergy analysis in the present study could also be applicable for diesel engine with other technology including EGR, turbo charging.

However, some investigations on exergy analysis of diesel engine with EGR and turbo charging were reported in literature. For instance, Rakopoulos and Giakoumis found that the irreversibility associated with turbocharger in diesel engine is about 4.7% of the

Table 5
Comparison of results from energy (First law) and exergy (Second law) balance at 75% load for diesel and dual-fuel mode (33.6% H_2 energy share).

S.No	Description	Energy (%)balance (first law)		Exergy (%) balance (second law)	
		Base diesel	Diesel + 33.6% H_2	Base diesel	Diesel + 33.6% H_2
1	Shaft power	30.93	35.25	28.31	30.73
2	Heat transfer loss	27.84	35.68	01.76	07.63
3	Exhaust gas loss	23.98	25.71	17.17	15.46
4	Unaccounted losses	17.25	03.36	–	–
5	Combustion irreversibility	–	–	15.46	12.17
6	Mixing irreversibility	–	–	08.42	08.18
7	Friction irreversibility	–	–	14.53	14.53
8	Unburned fuel irreversibility	–	–	14.35	11.30
9	Total (%)	100.00	100.00	100.00	100.00

total irreversibility [49]. With turbo charger, both heat transfer availability through cylinder walls and total irreversibility decrease marginally [36]. Zheng and Caton reported decrease in work availability from 36.6% with base diesel to 34.6% with 42% EGR and retarded fuel injection timing of 1.5° ATDC in a diesel engine (115 kW) at 1400 rpm [50]. It may be noted that work availability decreases with EGR technique but H_2 addition in the diesel engine (dual-fuel operation) enhances the work availability from 28.3% with base diesel to 30.7% with 33.6% H_2 energy share in the present study.

4.3.1. Effect of H_2 addition on CO_2 emission

Fig. 10 shows CO_2 emission from the H_2 diesel dual-fuel engine at different loads and constant engine speed of 1500 rpm. It is seen from the figure that CO_2 emission decreased drastically with increasing H_2

Table 6
Summary of first and second law of thermodynamics applied to H_2 dual-fuel diesel engine.

First law of thermodynamics		Second law of thermodynamics	
Input			
$E_{f,in} = \dot{m}_{f1} \times CV_{f1} + \dot{m}_{f2} \times CV_{f2}$	(1)	$A_{f,in} = a_1 \times \hat{g}f1(T_0, P_0) + b_1 \times \hat{g}_{f2(T_0,P_0)} + c_1 \times \hat{g}O_{2(T_0,P_0)} - \left[d_1 \times \hat{g}CO_{2(} \times \hat{g}H_2O_{(T_0,P_0)}\right] + R_u \times T_0 \times \ln\left\{(\dot{x}_{O_2})^{c1} / \left[(\dot{x}_{CO_2})^{d1} \times (\dot{x}_{H_2O})^{d2}\right]\right\}\}$	(25)
Output and losses			
$P_{s,out} = (2 \times \pi \times N \times T_r)/60$	(2)	$A_{s,out}/d\theta = \int_1^2 (p - p_0) \times \frac{dv}{d\theta}$	(29)
$E_{exh,out} = \left(\dot{m}_{f1} + \dot{m}_{f2}\right) \times (1 + AF) \times C_{p\ exh,out} \times (T_{exh,out} - T_0)$	(3)	$A_{exh,out} = \sum x_i\{h_i(T) - h_i(T_0) - T_0[s_i(T) - s_i(T_0)]\} + \sum R_u T_0 \ln\left(\frac{x_i p}{x_{io} p_0}\right)$	(31)
$Q_{convection1,out} = h_c \times A_r \times (T_g - T_{iw})$	(5)	$A_{Q_{t,out}} = \int_1^2 Q_{t,out} \times \left(1 - \frac{T_0}{T_g}\right)$	(30)
$Q_{convection,out} = K \times A_r \times (T_{iw} - T_{ow})$	(6)	$I_{mixing} = -R_u \times T_0 \times \sum_i \dot{m}_i \times \sum_i n_i \times \sum_i (x_i \times \ln(x_i))$	(38)
$Q_{convection2,out} = h_c \times A_r \times (T_{ow} - T_0)$	(7)	$I_{combustion} = T_0 \times \sum_{fi} \dot{m}_i \times \left\{s_o + C_p \ln\left(\frac{T}{T_0}\right) - R_u \ln\left(\frac{P}{P_0}\right)\right\}$	(39)
$Q_{radiation,out} = b_z \times \left(T_g^4 - T_0^4\right)$	(8)	$Q_{radiation,out} = b_z \times \left(T_g^4 - T_0^4\right) I_{unburned} = \oint \left(d\dot{m}_{unburned} \times A_{f,in}\right) d\theta$	(40)
$E_{unaccount,out} = E_{f,in} - (P_{s,out} + E_{exh,out} + Q_{t,out})$	(15)	$fp(\theta) = \mu \times \left\{\frac{\pi LN}{60} \mathrm{Sin}\,\theta \left[\frac{\mathrm{Cos}\,\theta}{\sqrt{R_l^2 - \mathrm{Sin}^2\theta}} - 1\right]\right\}^2$	(41)
		$I_{friction} = FP_u(\theta) = \oint fp_{(\theta)} d\theta$	(42)
		$I_t = I_{mixing} + I_{combustion} + I_{unburned} + I_{friction}$	(43)

energy share. The reason for the emission reduction is mainly due to decrease in carbon content in the fuel and energy efficiency improvement. Hydrogen has high flame velocity which enhances degree of constant volume combustion resulting to better combustion and energy efficiency. CO_2 emission decreased from 763 g/kWh with base diesel to 490 g/kWh with 18% H_2 energy share at rated load.

4.3.2. Effect of H_2 addition on PM and other emissions

Fig. 11 shows smoke (PM), HC, and CO emissions from the dual-fuel engine at rated load and constant engine speed of 1500 rpm with varying H_2 energy share. It can be observed from the figure that the smoke emission decreases substantially with increasing H_2 energy share. It decreased from 17.3% opacity with conventional diesel operation to 3% opacity with 18% H_2 energy share under dual-fuel operation. This could be postulated that with addition of H_2 gas, degree of homogeneity in the air–fuel mixture increases that leads to better combustion and low smoke emission. HC and CO emissions also decreased to almost zero level with the addition of H_2 along with diesel fuel. As H_2 is a carbon free energy carrier, it decreases all carbon-based emission significantly as seen in the figure. However, NO_x emission increased from 8.6 g/kWh with base diesel to 11.3 g/kWh with 18% H_2 energy share, but it can be reduced by using suitable technology including selective catalytic reduction technique. Hydrogen addition to the CI engine under dual-fuel mode is an effective solution to reduce all carbon-based emissions. As H_2 can be derived from variety of resources including renewable sources (solar and wind), H_2 utilization in CI engines under dual-fuel mode is a feasible option in near future.

5. Conclusions

The following conclusions are drawn based on results of this study. The exergy results of the diesel engine under dual-fuel mode (diesel–H_2) are compared with conventional mode (base diesel).

- Work availability of the diesel engine is higher with H_2 at all loads due to decrease in irreversibility of combustion and unburned fuel. It increased from 28% with base diesel to 31% with H_2 whereas irreversibility of combustion and unburned fuel decreased from 15.5% to 16.4% with base diesel to 12% and 11.3% with 33.6% H_2 energy share at 75% load and 1500 rpm. As exhaust gas availability increases with H_2 addition, more work can be extracted from exhaust gas energy.
- There is no effect of frictional power on maximum available work with H_2 as it is generally dependent on speed of the engine.
- Irreversibility of mixing process decreases slightly with H_2 addition (from 2.07 kW to 1.9 kW at 75% load).
- Both energy efficiency improvement and carbon content reduction in fuel result in drastic reduction in CO_2 emission which decreased from 838 g/kWh with base diesel to 483 g/kWh with 33.6% H_2 energy share under dual-fuel operation at 75% load.
- An important conclusion is emerged from the study that maximum available work and energy efficiency of the diesel engine increase with H_2 (dual-fuel mode) due to the irreversibility reduction in mainly combustion and unburned fuel. Further increase of H_2 energy share in the diesel engine would enhance maximum available work and reduce total irreversibility significantly. The other emissions (PM, CO, and HC) from the diesel engine decreased significantly with H_2.

Nomenclature

$\frac{\partial q}{\partial x_1}, \frac{\partial q}{\partial x_2}, \ldots, \frac{\partial q}{\partial x_n}$	partial differential of calculated parameter q which depends on different measured variables $x_1, x_2, \ldots, x_n$.
μ	coefficient of friction
A	availability, kW
a_1,b_1	molar fractions of fuels
ABDC	after bottom dead center
AF	air–fuel ratio
A_r	area of the cylinder, m^2
ATDC	after top dead center
B	bore, mm
BBDC	before bottom dead center
BTDC	before top dead center
b_z	Stefan–Boltzmann constant
C	carbon atom
c_1, d_1, d_2, and d_3	number of moles of air, CO_2, H_2O and N_2
CA	crank angle
CI	compression ignition
CO	Carbon monoxide
CO_2	carbon dioxide
C_p	specific heat at constant pressure, kJ/kg K
CR	compression ratio
CV	calorific value, kJ/kg
E	energy, kW
E_a	activation energy, mJ
EGR	exhaust gas recirculation
EPA	environmental protection agency
f_p	frictional power, kW
FP_u	total cyclic frictional power, kW
G	mass specific Gibbs free energy
$\hat{g}$	molar specific Gibbs free energy
H	hydrogen atom
h	specific enthalpy, kJ/kg
H_2	hydrogen gas
H_2O	water
h_c	convective heat transfer coefficient, W/m^2 K
HC	hydro carbon
I	irreversibility, kW
IC	internal combustion
K	thermal conductivity, W/m K
k_1, k_2, k_3	constants
L	stroke length, mm
$\dot{m}$	mass flow rate of fluids/species, kg/s
$\dot{M}$	molar flow rate
MW	molecular weight
N	engine speed, rpm
n	number of moles
N_2	nitrogen
NG	natural gas
NO_x	oxides of nitrogen
θ	degree crank angle
O	oxygen atom
O_2	oxygen
ORC	organic rankine cycle
P	power, kW
p	pressure, bar
PM	particulate matter
PM10	particulate matter with an aerodynamic diameter less than or equal to a nominal 10 μm
PM2.5	particulate matter with an aerodynamic diameter less than or equal to a nominal 2.5 μm
Pr	products
q	$f(x_1, x_2, \ldots, x_n)$ (q is the function of $x_1, x_2, \ldots, x_n$)
Q	heat transfer, kW
R	reactants
R_l	ratio of connecting rod length to crank radius
rpm	rotations per minute
RR	reaction rate

R_u	universal gas constant
s	specific entropy, kJ/kg K
SEC	specific energy consumption, MJ/kW h
SOI	start of injection
T	temperature, K
T_r	torque, N m
V	velocity, m/s
v	volume, m^3
$\dot{x}$	mass fraction
x	molar fraction
$x_1, x_2,\ldots,x_n$	measured variables
$\Delta x_1, \Delta x_2,\ldots,\Delta x_n$	fluctuation of respective measured variables x_1, $x_2,\ldots,x_n$.

Suffixes

0	dead state
a	air
exh	exhaust
f	fuel
f1	fuel 1 (Euro IV diesel)
f2	fuel 2 (hydrogen)
g	gas
i	species
in	input
iw	inside of cylinder wall
out	output
ow	outside of cylinder wall
s	shaft
t	total
α_1	number of carbon atoms in fuel 1
α_2	number of carbon atoms in fuel 2
β_1	number of hydrogen atoms in fuel 1
β_2	number of hydrogen atoms in fuel 2

References

[1] Road sector diesel fuel consumption per capita (kg of oil equivalent). www.data.worldbank.org/indicator/IS.ROD.DESL.PC/countries?display=graph [accessed 13.04.13].

[2] World Diesel Engines to 2015 - Demand and Sales Forecasts, Market Share, Market Size, Market Leaders. Study No. 2864 World diesel engines to 2015 – Demand and Sales Forecasts, Market share, Market size, Market Leaders. pp. 235–324., www.freedoniagroup.com/World-Diesel-Engines.html; 2012 [accessed 10.04.13].

[3] Policy assessment for the review of the particulate matter national ambient air quality standards figure captions. U.S. Environmental Protection Agency, Office of Air Quality Planning and Standards; April 2011. EPA 452/R-11-003, www.epa.gov/ttn/naaqs/standards/pm/data/20110419pmpafinal.pdf [accessed 07.06.13].

[4] Regulation (EC) No. 715/2007 of the European Parliament and of the Council of 20 June 2007.http://eur-lex.europa.eu/LexUriServ/LexUriServ.do?uri=OJ:L:2007:171:0001:0001:EN:PDF; 2007 [accessed 07.06.13].

[5] Regulation (EC) No. 443/2009 of the European Parliament and Council 23 April 2009.http://eur-lex.europa.eu/LexUriServ/LexUriServ.do?uri=OJ:L:2009:140:0063:008:EN:PDF; 2009 [accessed 21.02.13].

[6] Primary CI engine CO_2, N_2O and CH_4 emissions standards. Code of Federal regulations, 40 CFR Part 1036.108. www.epa.gov/otaq/climate/regulations.htm. [accessed 21.02.13].

[7] Tsolakis A, Hernandez JJ, Megaritis A, Crampton M. Dual-fuel diesel engine operation using H_2 effect on particulate emissions. Energy Fuels 2005;19:418–25.

[8] Wu H-W, Wang R-H, Chen Y-C, Ou D-J, Chen T-Y. Influence of port-inducted ethanol or gasoline on combustion and emission of a closed cycle diesel engine. Energy 2014;64:259–67.

[9] Miyamoto T, Hirokazu H, Masato M, Naoya K, Hajime K, Yasuhiro U. Effect of hydrogen addition to intake gas on combustion and exhaust emission characteristics of a diesel engine. Int J Hydrog Energy 2011;36:13138–49.

[10] Chintala V, Subramanian KA. A CFD (computational fluid dynamics) study for optimization of gas injector orientation for performance improvement of a dual-fuel diesel engine. Energy 2013;57:709–21.

[11] National hydrogen Energy road map – 2006 (abridged version, 2007). Path way for transition to hydrogen energy for India. National Hydrogen Energy Board, Ministry of New and Renewable Energy, Government of India; 2006.http://mnre.gov.in/file-manager/UserFiles/abridged-nherm.pdf [accessed 23.03.13].

[12] Dunbar WR, Lior N. Sources of combustion irreversibility. Combust Sci Technol 1994;103:41–61.

[13] Caton JA. On the destruction of availability (exergy) due to combustion processes with specific application to internal-combustion engines. Energy 2000;25:1097–117.

[14] Rakopoulos CD, Kyritsis DC. Comparative second-law analysis of internal combustion engine operation for methane, methanol, and dodecane fuels. Energy 2001;26:705–22.

[15] Rakopoulos CD, Scott MA, Kyritsis DC, Giakoumis EG. Availability analysis of hydrogen/natural gas blends combustion in internal combustion engines. Energy 2008;33:248–55.

[16] Jonathan N, Dincer I. Comparative exergy analysis of gasoline and hydrogen fueled ICEs. Int J Hydrog energy 2010;35:5124–32.

[17] Taymaz I. An experimental study of energy balance in low heat rejection diesel engine. Energy 2006;31:364–71.

[18] Shu G, Jian Z, Hua T, Xingyu L, Haiqiao W. Parametric and exergetic analysis of waste heat recovery system based on thermoelectric generator and organic rankine cycle utilizing R123. Energy 2012;45:806–16.

[19] Ghazikhani M, Hatami M, Ganji DD, Gorji-Bandpy M, Behravan A, Shahi G. Exergy recovery from the exhaust cooling in a DI diesel engine for BSFC reduction purposes. Energy 2014;65:44–51.

[20] Fu J, Liu J, Ren C, Wang L, Deng B, Xu Z. An open steam power cycle used for IC engine exhaust gas energy recovery. Energy 2012;44:544–54.

[21] Fu J, Liu J, Xu Z, Ren C, Deng B. A combined thermodynamic cycle based on methanol dissociation for IC (internal combustion) engine exhaust heat recovery. Energy 2013;55:778–86.

[22] Domingues A, Helder S, Costa M. Analysis of vehicle exhaust waste heat recovery potential using a Rankine cycle. Energy 2013;49:71–85.

[23] Byung CC, Young MK. Thermodynamic analysis of a dual loop heat recovery system with trilateral cycle applied to exhaust gases of internal combustion engine for propulsion of the 6800 TEU container ship. Energy 2013;58:404–16.

[24] Jannelli E, Minutillo M, Cozzolino R, Falcucci G. Thermodynamic performance assessment of a small size CCHP (combined cooling heating and power) system with numerical models. Energy 2014;65:240–9.

[25] Larsen U, Nguyen TV, Knudsen T, Haglind F. System analysis and optimization of a Kalina split-cycle for waste heat recovery on large marine diesel engines. Energy 2014;64:484–94.

[26] Kalyan KS, Pedro JM, Sundar RK. Analysis of exhaust waste heat recovery from a dual-fuel low temperature combustion engine using an organic Rankine cycle. Energy 2010;35:2387–99.

[27] Yu G, Shu G, Hua T, Haiqiao W, Lina L. Simulation and thermodynamic analysis of a bottoming organic Rankine cycle (ORC) of diesel engine (DE). Energy 2013;51:281–90.

[28] Sarabchi N, Khoshbakhti SR, Mahmoudi SMS. Utilization of waste heat from a HCCI (homogeneous charge compression ignition) engine in a tri-generation system. Energy 2013;55:965–76.

[29] Livio DS, Gianluigi LB, Daniele B. Energy characterization of CHP (combined heat and power) fuelled with hydrogen enriched natural gas blends. Energy 2013;60:13–22.

[30] Amjad AK, Khoshbakhi SR, Mahmoudi SMS, Rahimi A. Availability analysis of n-heptane and natural gas blends combustion in HCCI engines. Energy 2011;36:6900–9.

[31] Yoge JRC, Antonio GBL, Celso RBF, Araujo LL. Energetic and exergetic analysis of a dual-fuel diesel engine. Renew Sustain Energy Rev 2012;16:4651–60.

[32] Harilal SS, Hitesh JY. Energy analysis to a CI-engine using diesel and bio-gas dual-fuel – a review study. Int J Adv Eng Res Stud 2012;1(2):212–7.

[33] Sahoo BB, Ujjwal KS, Sahoo N. Theoretical performance limits of a syngas-diesel fueled compression ignition engine from second law analysis. Energy 2011;36:760–9.

[34] Woshchni G. A universally applicable equation for the instantaneous heat transfer coefficient in the internal combustion engine. SAE Paper No. 670931; 1967.

[35] Borman GL, Ragland KW. Combustion engineering. WCB/McGraw-Hill International Editions; 1998, ISBN 0-07-115978-9; 1998.

[36] Parlak A. The effect of heat transfer on performance of the diesel cycle and exergy of the exhaust gas stream in a LHR diesel engine at the optimum injection timing. Energy Convers Manag 2005;46:167–79.

[37] Lakshmanan T, Nagarajan G. Experimental investigation of timed manifold injection of acetylene in direct injection diesel engine in dual-fuel mode. Energy 2010;35:3172–8.

[38] Horng WW, Zhan YW. Combustion characteristics and optimal factors determination with Taguchi method for diesel engines port-injecting hydrogen. Energy 2012;47:411–20.

[39] Prins MJ, Ptasinski KJ. Energy and exergy analysis of the oxidation and gasification of carbon. Energy 2005;30:982–1002.

[40] Salehzadeh A, Khoshbakhti SR, Jalali VD. Investigating the effect of several thermodynamic parameters on exergy destruction in components of a tri-generation cycle. Energy 2013;52:96–109.

[41] Hongqing F, Huijie L. Second-law analyses applied to a spark ignition engine under surrogate fuels for gasoline. Energy 2010;35:3551–6.

[42] Rakopoulos CD, Michos CN, Giakoumis EG. Availability analysis of a syngas fueled spark ignition engine using a multi-zone combustion model. Energy 2008;33:1378–98.

[43] Alta AK, Kalyan KS, Sundar RK, Stephen AC. Fuel and diluent effects on entropy generation in a constant internal energy-volume (UV) combustion process. Energy 2012;43:315–28.

[44] Antusch S, Dienwiebel M, Nold E, Albers P, Spichera U, Scherge M. On the tribochemical action of engine soot. Wear 2010;269:1–12.
[45] Truhan JJ, Qub J, Blau PJ. The effect of lubricating oil condition on the friction and wear of piston ring and cylinder liner materials in a reciprocating bench test. Wear 2005;259:1048–55.
[46] Staley D. Correlating lube oil filtration efficiencies with engine wear. SAE Paper No. 881825; 1988.
[47] Green DA, Lewis R, Dwyer-Joyce RS. Wear effects and mechanisms of soot-contaminated automotive lubricants. Proc Inst Mech Eng J Eng Tribol 2006;220(3):159–69.
[48] Rakopoulos CD, Giakoumis EG. Speed and load effects on the availability balances and irreversibilities production in a multi-cylinder turbocharged diesel engine. Appl Therm Eng 1997;17(3):299–313.
[49] Rakopoulos CD, Giakoumis EG. Availability analysis of a turbocharged diesel engine operating under transient load conditions. Energy 2004;29:1085–104.
[50] Zheng J, Caton JA. Second law analysis of a low temperature combustion diesel engine: effect of injection timing and exhaust gas recirculation. Energy 2012;38:78–84.